NASA CONTRACTOR REPORT

NASA CR-1125

NASA CR-1125

HYDRODYNAMICS OF AIRCRAFT TIRE HYDROPLANING

by S. Tsakonas, C. J. Henry, and W. R. Jacobs

Prepared by
STEVENS INSTITUTE OF TECHNOLOGY
Hoboken, N. J.
for

NATIONAL AERONAUTICS AND SPACE ADMINISTRATION • WASHINGTON, D. C. • AUGUST 1968

NASA CR-1125

HYDRODYNAMICS OF AIRCRAFT TIRE HYDROPLANING

By S. Tsakonas, C. J. Henry,
and W. R. Jacobs

Distribution of this report is provided in the interest of information exchange. Responsibility for the contents resides in the author or organization that prepared it.

Issued by Originator as Report No. 1238

Prepared under Contract No. NSR 31-003-016 by
STEVENS INSTITUTE OF TECHNOLOGY
Hoboken, N.J.

for

NATIONAL AERONAUTICS AND SPACE ADMINISTRATION

For sale by the Clearinghouse for Federal Scientific and Technical Information
Springfield, Virginia 22151 – CFSTI price $3.00

ABSTRACT

An approximate theory has been developed for a study of the hydroplaning tire by considering it as a planing surface of small aspect ratio in extremely shallow water. The results of this approximation exhibit hydrodynamic behavior similar to that of hydroplaning pneumatic tires and thus indicate that the tire hydroplaning phenomenon can be described from the standpoint of inviscid hydrodynamics. The analysis furnishes families of curves which can be considered to represent, qualitatively, the start of hydroplaning and thus give qualitative guidance for avoiding the undesirable hydroplaning condition.

TABLE OF CONTENTS

NOMENCLATURE

$A = \frac{\ell}{b}$	aspect ratio of planing surface
b	half-length of wetted surface of plate
b_1	longitudinal dimension of footprint from wheel axle to trailing edge
b_2	longitudinal dimension of footprint from wheel axle to leading edge
C_L	coefficient of total lift defined in Eq. (37)
d	clearance of trailing edge of tire wetted surface from ground
$F_i(A)$	functions defined in Eq. (38)
h	depth of water on runway or ground
$K_{ij}(\ )$	kernel function representing induced velocity on element j due to unit amplitude load on element i
L	total lift on hydroplaning tire
L_G	loading on ground
L_T	loading on tire
L'	cumulative loading distribution
ℓ	half-width of footprint and of wetted surface of tire
n	index of summation
p_o	tire inflation pressure
S	lifting surface
U	forward velocity of vehicle
$u(\ )$	unit step function
W_G	downwash velocity distribution normal to ground
W_T	downwash velocity distribution normal to tire

x_G, y_G, h	coordinates of control point on ground
x_T, y_T, 0	coordinates of control point on tire wetted surface
$x_{ij} = x_i - \xi_j$	
$y_{ij} = y_i - \eta_j$	
y'	chordwise variable of integration
$z(x,y)$	camber of tire surface
$\beta = \frac{dz}{dx}$	angle of attack of planing surface
θ	angular chordwise location
Λ_i	various integrals
λ_i	defined in (29) and (30)
ξ_G, η_G, h	coordinates of loading point on ground
ξ_T, η_T, 0	coordinates of loading point on tire surface
ρ	mass density of fluid
φ	angular chordwise location
Ψ	function (see Eqs. (15) and (16))
ψ	defined in (31)

INTRODUCTION

Pneumatic tires rolling on a wet runway may reach a speed where the tire becomes completely detached from the ground and skids along on a thin film of water. At that stage, directional stability and control, as well as braking traction, are completely lost. When tire and surface are no longer in contact, the tire is said to be hydroplaning. It no longer rolls but slides without control across the surface.

A series of theoretical studies has been made, based on one of the fundamental assumptions, either that the hydroplaning phenomenon could be reasonably explained in terms of fluid density alone (hydrodynamic pressure)[1,2] or that it is basically one of lubrication.[3] At the same time experimental studies[4,5,6] have been conducted in an effort to reveal the physical mechanism of the hydroplaning tire as well as the important parameters affecting the phenomenon.

Admittedly the tire-hydroplaning phenomenon is quite complicated. Perhaps at one stage the hydrodynamic aspects of the phenomenon are dominated by viscous effects (hence lubrication), at another by inertia effects and at a later stage by thermodynamic effects (reversion of the rubber and formation of steam pocket). At each and every stage, of course, the elastic properties of tires and their texture and geometry, as well as the relative roughness of the wet pavement, enter into the problem.

For those cases of hydroplaning where velocity is quite high and the water is relatively deep, it seems rather reasonable to assume that the viscosity effects become insignificant[1] for such high Reynolds numbers as exist at that stage.

The present study has been based on the premise that the fluid inertia effect is the predominant property. The three-dimensional character of the phenomenon has been preserved and the effects on tire hydroplaning will be obtained due to aspect ratio and shape of the planing surface and to depth of water, together with vehicle speed. The general formulation of the hydrodynamic aspect of the non-viscous hydroplaning problem leads to a pair of surface integral equations with unknown loading distribution on the tire and on the ground. However, due to the limitations of the contract for this initial study an approximate solution will be obtained based on the following assumptions: a) the tire is regarded as a low-aspect ratio lifting surface, b) the pressure distribution on the pavement is approximated by a step function of magnitude given by experimental measurements. The results of this initial investigation indicate that the approximate solution correctly predicts the trend but not the magnitude of the hydrodynamic lift and confirms qualitatively the important characteristics observed in the tire-hydroplaning phenomenon. For future studies it is recommended to improve the mathematical model so that the three-dimensional non-viscous contribution may be defined as accurately as possible and then the elasticity of the tire may be incorporated.

THEORY

At the stage of complete detachment of the hydroplaning tire from the wet pavement, the contact area of the tire is assumed to have infinite radius of curvature as shown in Figure 1 and at that stage the total weight of the vehicle will be sustained by the hydrodynamic pressure distribution developed in the film of water between the tire and the ground. This situation is simulated by a mathematical model presented in Figure 2, where the area of tire in contact with the fluid will be considered as a lifting surface of finite aspect ratio planing at the free surface of extremely shallow water at high Froude number, since the vehicle speed is considered very high.

The right-handed cartesian coordinate system is selected with positive x-axis in the direction of fluid motion (opposite that of vehicle) and positive z-axis in the downward direction. The present study utilizes the linearized lifting surface theory which is based on a small perturbation approximation together with the assumption of thin surfaces in uniform flow of an incompressible inviscid fluid.

The pressure field generated by a lifting surface S has been shown to be given by distributed doublets with axis parallel to the local normal and strength proportional to the pressure jump across the surface S. If these unknown loadings on the tire and ground are designatd by $L_T(\xi_T,\eta_T)$ and $L_G(\xi_G,\eta_G)$ respectively, then the kinematic conditions which exist at both lifting surfaces (tire plane and ground) will be expressed mathematically on the basis of linear approximation (i.e., small perturbation theory) as follows:

$$W_T(x_T,y_T,0) = \frac{1}{4\pi\rho U} \iint_{S_T} L_T(\xi_T,\eta_T)\ K_{TT}(x_T,y_T,0;\xi_T,\eta_T,0)dS_T$$

$$+ \frac{1}{4\pi\rho U} \iint_{-\infty}^{\infty} L_G(\xi_G,\eta_G)\ K_{GT}(x_T,y_T,0;\xi_G,\eta_G,h)dS_G \qquad (1)$$

$$W_G(x_G,y_G,h) = \frac{1}{4\pi\rho U} \iint_{S_T} L_T(\xi_T,\eta_T)\; K_{TG}(x_G,y_G,h;\xi_T,\eta_T,0)\,dS_T$$

$$+ \frac{1}{4\pi\rho U} \int_{-\infty}^{\infty}\!\!\int L_G(\xi_G,\eta_G)\; K_{GG}(x_G,y_G,h;\xi_G,\eta_G,h)\,dS_G \qquad (2)$$

where $(x_T,\ y_T,\ 0)$

and $(\xi_T,\ \eta_T,\ 0)$ = coordinates of control and loading point, respectively, located on the tire surface

(x_G,y_G,h) and (ξ_G,η_G,h) coordinates of control and loading point, respectively, located on the ground plate

$W_T(\ )$ and $W_G(\ )$ the known downwash velocity distribution normal to the tire and ground plate, respectively

$K_{ij}(\ )$ kernel function which represents the induced velocity on an element j due to a unit amplitude load on element i. Subscripts i and j designate tire or ground plate.

For the case of rigid plates the known downwash distribution will be given by

$$W_T(x_T,y_T,0) \approx -\ U\,\frac{\partial z}{\partial x} \qquad (3)$$

and

$$W_G(x_G,y_G,h) = 0$$

where the first expresses the fact that the flow remains always tangent to the tire surface which has camber given by z(x,y), and the second imposes the same requirement at the ground which has been assumed to be flat.

The two equations (1) and (2) constitute a pair of surface integral equations with the unknown loading functions $L_T(\xi_T,\eta_T)$ and $L_G(\xi_G,\eta_G)$ to be determined in terms of specified velocity distributions. It should be noted that this formulation can accommodate any downwash velocity distribution, even that for the elastic tire.

The development of the various kernel functions is omitted in the present study since it can be easily obtained from Reference 7. In fact, K_{TT} is obtained from Equation (74) in that reference by putting d = h = 0, K_{GG} from Equation (75) for d = h, and the rest are obtained in a fashion similar to that given in Reference 7.

Because tire hydroplaning is considered a high-speed phenomenon, these kernel functions are determined at high Froude number so that the free surface effect is considered to be equivalent to that of the "bi-plane" where the velocity potential acquires zero value at the free surface. The bottom effect is taken into account as the usual "wall effect."

Thus the kernel functions are given by

$$K_{TT} = \frac{2}{y_{TT}^2}\left[1 + \frac{x_{TT}}{x_{TT}^2 + y_{TT}^2}\right] \tag{4}$$

$$K_{GG} = \frac{1}{y_{GG}^2}\left[1 + \frac{x_{GG}}{\sqrt{x_{GG}^2 + y_{GG}^2}}\right] + \frac{1}{y_{GG}^2 + (2h)^2}\left[1 + \frac{x_{GG}}{\sqrt{x_{GG}^2 + y_{GG}^2 + (2h)^2}}\right]$$
$$- \frac{(2h)^2}{\left[y_{GG}^2 + (2h)^2\right]^2}\left\{\frac{x_{GG}}{\sqrt{x_{GG}^2 + y_{GG}^2}}\left[2 + \frac{y_{GG}^2 + (2h)^2}{x_{GG}^2 + y_{GG}^2 + (2h)^2}\right] + 2\right\} \tag{5}$$

$$K_{GT} = -\frac{2}{y_{TG}^2 + h^2}\left\{\left(1 - \frac{3h^2}{y_{TG}^2 + h^2}\right)\frac{x_{TG}}{\sqrt{x_{TG}^2 + y_{TG}^2 + h^2}}\right.$$
$$\left. - \frac{h^2}{y_{TG}^2 + h^2}\left(2 - \frac{x_{TG}}{\left[x_{TG}^2 + y_{TG}^2 + h^2\right]^{3/2}}\right) + 1\right\} \tag{6}$$

and

$$K_{TG} = -\frac{2}{y_{GT}^2 + h^2}\left\{\left(1 - \frac{3h^2}{y_{GT}^2 + h^2}\right)\frac{x_{GT}}{\sqrt{x_{GT}^2 + y_{GT}^2 + h^2}}\right.$$

$$\left. - \frac{h^2}{y_{GT}^2 + h^2}\left(2 - \frac{x_{GT}^3}{\left[x_{GT}^2 + y_{GT}^2 + h^2\right]^{3/2}}\right) + 1\right\} \qquad (7)$$

where

$$x_{TT} = x_T - \xi_T \qquad y_{TT} = y_T - \eta_T$$

$$x_{GG} = x_G - \xi_G \qquad y_{GG} = y_G - \eta_G$$

$$x_{TG} = x_T - \xi_G \qquad y_{TG} = y_T - \eta_G$$

$$x_{GT} = x_G - \xi_T \qquad y_{GT} = y_G - \eta_T$$

When Equations 3, 4, 5, 6, 7 are substituted in Equations 1 and 2, the pair of integral equations is brought to its desired working form. It should be noted that the kernel functions K_{TT} and K_{GG} which represent the self-induced velocity on a point of the lifting surface by a unit amplitude loading located on the same surface, have second order singularity whose "Hadamard" finite contribution can be extracted by means of Lagrange's Interpolation method.[7] An analytical solution of the pair of integral equations seems impossible in the present state-of-the-art, however, a numerical solution can be sought along the line suggested by Watkins, et al.[8] To apply this procedure, the loading functions are assumed made up of mode shapes dictated by certain physical considerations (leading and trailing edge and tip conditions) whose unknown coefficients will be determined by satisfying the boundary conditions at an equivalent number of control points on the lifting surfaces. This method is described as the "Mode Approach" in conjunction with the "Collocation Method."

But, in the present problem the extension of the ground plate to infinity excludes the possibility of utilizing the Birnbaum chordwise modes, viz., $(A_o \cot \frac{\theta}{2} + \sum_{n=1}^{\infty} A_n \sin n\theta)$, as well as the polynomial representation of the spanwise distribution with infinite slope at the tips. However, from experimental observations[4,5,6] it is seen that the pressure distribution on the ground at the time of hydroplaning of the tire is mainly confined within the footprint of the tire, outside of which the pressure decays extremely fast. It appears that this fundamental characteristic of the ground pressure should be incorporated into the problem. This can be easily achieved by proper combination of unit step functions. Thus the step function will be considered as the fundamental mode in both chordwise and spanwise directions, on which sinusoidal modes with proper decay factor can be superimposed to give the detailed pressure distribution on the ground plate.

Such mode shapes for the ground pressure are conjectural and hence a careful and systematic study must be undertaken. However, as a first attempt the "step-like" mode shapes in both chordwise and spanwise direction are considered advisable and realistic.

SIMPLIFIED MATHEMATICAL MODEL

A) Ground Pressure Distribution

In accordance with the previous discussions and in conformity with experimental observation, the pressure distribution on the ground plate will be assumed to be approximated by a step-type function, asymmetrically extended about the center of the original footprint of the pneumatic tire, with intensity equal to the tire inflation pressure p_o (see Figure 3A).

Thus the pressure distribution on the ground plate will be given by

$$L_G(\xi_G,\eta_G) = + 2p_o\left[u(\xi + b_2) - u(\xi - b_1)\right]\left[u(\eta + \ell) - u(\eta - \ell)\right] \qquad (8)$$

where u( ) is unit step function. By insertion of a factor of 2 it is stipulated that the pressure jump across the lifting surface (i.e., ground plate) is in fact, double the pressure on one side of the surface.

It is obvious then that, in effect, the pair of integral equations is reduced to a single integral equation (Eq. 1) with unknown loading function on the planing tire. In fact the integral equation which will be solved is

$$-U\beta = \frac{1}{4\pi\rho U}\iint_{S_T} L_T(\xi_T,\eta_T)\, K_{TT}(x_y,y_T,0;\xi_T,\eta_T,0)d\xi_T\, d\eta_T$$

$$+ \frac{p_o}{2\pi\rho U}\int_{-\infty}^{\infty}\int \left[u(\xi_G+b_2) - u(\xi_G-b_1)\right]\left[u(\eta_G+\ell) - u(\eta_G-\ell)\right]K_{GT}\left(x_T,y_T,0;\xi_G,\eta_G,0\right]d\xi_G d\eta_G$$

where K_{TT} and K_{GT} are given by Eqs. 4 and 6 and $-U\beta$ is the slope of the planing surface to the horizontal plane (see Eq. 3).

The integral equation reduces to:

$$\frac{1}{2\pi\rho U}\int_{-\ell}^{\ell}\int_{-b}^{b}\frac{L_T(\xi_T,\eta_T)}{y_{TT}^2}\left\{1+\frac{x_{TT}}{\sqrt{x_{TT}^2+y_{TT}^2}}\right\}d\xi_T\,d\eta_T = W(x_T,y_T) \tag{9}$$

where

$$W(x_T,y_T) = -U\beta + \frac{p_o}{\pi\rho U}\int_{-\ell}^{\ell}\int_{-b_2}^{b_1}\frac{1}{y_{TG}^2+h^2}\left\{\left(1-\frac{3h^2}{y_{TG}^2+h^2}\right)\frac{x_{TG}}{\sqrt{x_{TG}^2+y_{TG}^2+h^2}}\right.$$

$$\left. -\frac{h^2}{y_{TG}^2+h^2}\left(2-\frac{x_{TG}^3}{(x_{TG}^2+y_{TG}^2+h^2)^{3/2}}\right)+1\right\}d\xi_T\,d\eta_T \tag{10}$$

is the downwash distribution plus the induced velocity at the planing tire due to the assumed ground pressure distribution.

Hence the unknown loading distribution $L_T(\xi_T,\beta_T)$ on the hydroplaning tire will be determined in terms of the angle of attack, β, (i.e., camber distribution $\beta = \partial z/\partial x$ and the induced velocity by the pressure patch on the ground.

B) Low Aspect Ratio Approximation

From the geometry of a typical tire footprint it can be surmised that the tire in the hydroplaning condition can be approximated by a low aspect ratio wing. Hence, it will be assumed that in the greatest portion of the lifting surface the spanwise distances $|y_T - \eta_T|$ have small magnitudes compared with chordwise distances $|x_T - \xi_T|$, i.e., most of the time the following condition

$$|y_T - \eta_T| < |x_T - \xi_T|$$

prevails.

Thus the kernel of the integral equation (see Eq. 9) is approximated by

$$\left[1 + \frac{x_T - \xi_T}{\sqrt{(x_T-\xi_T)^2 + (y_T-\eta_T)^2}}\right] \approx \left[1 + \frac{x_T - \xi_T}{|x_T - \xi_T|}\right] = \begin{cases} 2 \text{ for } \xi_T < x_T \\ 0 \text{ for } \xi_T > x_T \end{cases} \tag{11}$$

Upon substitution of Eq. (11), Eq. (9) becomes

$$\frac{1}{\pi \rho U} \int_{-b}^{x} \int_{-\ell}^{\ell} \frac{L_T(\xi_Y, \eta_T)}{(y_T - \eta_T)^2} \, d\eta_T \, d\xi_T = W(x_T, y_T) \tag{12}$$

This integral equation reflects the approximation that conditions at a given point on the planing tire are influenced only by what takes place upstream from that point.

On introducing the function $L_T^{\prime}(x_T, \eta_T)$ as the cumulative loading distribution defined by

$$\int_{-b}^{x_T} L_T(\xi_T, \eta_T) d\xi_T = L'(x_T, \eta_T) \tag{13}$$

the integral equation (12) becomes

$$-\frac{1}{\pi} \int_{-\ell}^{\ell} L'(x_T, \eta_T) \frac{\partial}{\partial y_T} \left(\frac{1}{y_T - \eta_T}\right) d\eta_T = \rho U W(x_T, y_T) \tag{14}$$

whose inversion is given by (see Appendix A)

$$L'(x_T, y_T) = -\rho U \int_{-\ell}^{\ell} W(x_T, y') \, \Psi(y_T, y') dy' \tag{15}$$

where

$$\Psi(y_T, y') = \frac{1}{\pi} \ell n \left| \frac{\ell^2 - y_T y' - \sqrt{(\ell^2 - y_T^2)(\ell^2 - y'^2)}}{\ell(y' - y_T)} \right| \tag{16}$$

provided that the loading function $L'(x_T,n_T)$ vanishes at the tips, i.e.,

$$L'(x_T, -\ell) = L'(x_T, \ell) = 0 \quad .$$

The total lift developed on the hydroplaning tire will then be given by

$$L = \int_{-\ell}^{\ell} L'(b,y_T)dy_T$$

or

$$L = -\rho U \int_{-\ell}^{\ell}\int_{-\ell}^{\ell} W(b,y')\ \Psi(y_T,y')dy'\ dy_T \ . \tag{17}$$

It should be noted that the above solution of the integral equation (12) should be considered as the first approximation of the solution of the more general integral equation (9) which incorporates the full-fledged finite aspect ratio effect. This can be easily seen by writing Equation 9 in the following form

$$\frac{1}{\pi}\int_{-\ell}^{\ell}\int_{-b}^{b} \frac{L_T(\xi_T,\eta_T)}{y_{TT}^2}\ d\xi_T\ d\eta_T = 2\rho UW(x_T,y_T) - \frac{1}{\pi}\int_{-\ell}^{\ell}\int_{-b}^{b} \frac{L_T(\xi_T,\eta_T)}{y_{TT}^2}\ \frac{x_{TT}}{\sqrt{x_{TT}^2+y_{TT}^2}}\ d\xi_T\ d\eta_T$$

which upon multiplication by the function $\Psi(y,y')$ and integration from $-\ell$ to ℓ (see Appendix B) yields

$$L'(x_T,y_T) = \frac{2\rho U}{\pi}\int_{-\ell}^{\ell} W(x_T,y')\ \Psi(y,y')dy' - \frac{1}{\pi^2}\int_{-\ell}^{\ell}\int_{-b}^{b} L'(\xi_T,\eta_T)\ K(x_T,y_T;\xi_T\eta_T)d\xi_T d\eta_T$$

where

$$K(x_T,y_T;\xi_T,\eta_T) = \int_{-\ell}^{\ell} \frac{\Psi(y_T,y')\ dy'}{\left[(x_T-\xi_T)^2 + (y'-\eta_T)^2\right]^{3/2}} \tag{18}$$

Equation (18) is a Fredholm integral equation of the second kind with unknown $L'(\xi_T,\eta_T)$.

In the present preliminary study, however, the assumption that the tire at the hydroplaning stage is a low aspect ratio lifting surface will be utilized and hence the integral equation given by Eq. 12 with its corresponding solution given by Eq. 15 will be considered the fundamental relation to be used. The integral equation (18) will be left for possible future studies.

C) Evaluation of the Ground-Induced Velocity

The downwash distribution at the planing tire is given by Eq. 10 whose first term represents the angle of attack condition and whose second term the velocity induced by the pressure distribution at the ground.

The downwash distribution (Eq. 10) is written as

$$W = W_1 + W_2 \tag{19}$$

where

$$W_1 = - U\beta$$

and

$$W_2 = + \frac{p_o}{\pi\rho U} \int_{-\ell}^{\ell}\int_{-b_2}^{b_1} \frac{1}{y_{TG}^2+h^2} \left\{ \left(1 - \frac{3h^2}{y_{TG}^2+h^2}\right) \frac{x_{TG}}{\sqrt{x_{TG}^2+y_{TG}^2}} - \frac{h^2}{y_{TG}^2+h^2} \left(2 - \frac{x_{TG}^3}{(x_{TG}^2+y_{TG}^2+h^2)^{3/2}}\right) + 1 \right\} d\xi_T d\eta_T \tag{20}$$

which after straight-forward integrations with respect to ξ_T and η_T yields

$$W_2 = \frac{-p_o}{\pi\rho U}\left\{\ell n \quad \frac{y_T+\ell+\sqrt{(y_T+\ell)^2+(x_T+b_2)^2+h^2}}{y_T-\ell+\sqrt{(y_T-\ell)^2+(y_T+b_2)^2+h^2}} \quad \frac{y_T-\ell+\sqrt{(y_T-\ell)^2+(x_T-b_1)^2+h^2}}{y_T+\ell+\sqrt{(y_T+\ell)^2+(x_T-b_1)^2+h^2}}\right.$$

$$+\frac{h^2/\sqrt{(x_T+\ell)^2+)x_T+b_2)^2+h^2}}{y_T+\ell+\sqrt{(x_T+\ell)^2+(x_T+b_2)^2+h^2}} - \frac{h^2/\sqrt{(y_T-\ell)^2+(x_T+b_2)+h^2}}{y_T-\ell+\sqrt{(y_T-\ell)^2+(x_T+b_2)^2+h^2}}$$

$$-\frac{h^2/\sqrt{(y_T+\ell)^2+(x_T-b_1)^2+h^2}}{y_T+\ell+\sqrt{(y_T+\ell)^2+(x_T-b_1)^2+h^2}} + \frac{h^2/\sqrt{(y_T-\ell)^2+(x_T-b_1)^2+h^2}}{y_T-\ell+\sqrt{(y_T-\ell)^2+(x_T-b_1)^2+h^2}}$$

$$-\frac{(x_T\ b_2)^2(y_T+\ell)\left[(y_T+\ell)^2+(x_T+b_2)^2+2h^2\right]}{\left\{h^2\left[(y_T+\ell)^2+(x_T+b_2)^2+h^2\right]+(y_T+\ell)^2(x_T+b_2)^2\right\}\sqrt{(y_T+\ell)^2+(y_T+b_2)^2+h^2}}$$

$$+\frac{(x_T+b_2)^2(y_T-\ell)\left[(y_T-\ell)^2+(x_T+b_2)^2+2h^2\right]}{\left\{h^2\left[(y_T-\ell)^2+(x_T+b_2^2)^2+h^2\right]+(y_T-\ell)^2(x_T+b_2)^2\right\}\sqrt{(x_T-\ell)^2+(x_T+b_2)^2+h^2}}$$

$$+\frac{(x_T-b_1)^2(y_T+\ell)\left[(y_T+\ell)^2+(x_T-b_1)^2+2h^2\right]}{\left\{h^2\left[(y_T+\ell)^2+(x_T-b_1)^2+b^2\right]+(y_T+\ell)^2(x_T-b_1)^2\right\}\sqrt{(y_T+\ell)^2+(x_T-b_1)^2+h^2}}$$

$$-\frac{(x_T-b_1)^2(y_T-\ell)\left[(y_T-\ell)^2+(x_T-b_1)^2+2h^2\right]}{\left\{h^2\left[(y_T-\ell)^2+(x_T-b_1)^2+h^2\right]+(y_T-\ell)^2(x_T-b_1)^2\right\}\sqrt{(y_T-\ell)^2+(x_T-b_1)^2+h^2}}$$

$$\left.-(b_1+b_2)\left[\frac{y_T+\ell}{y_T+\ell)^2+h^2}-\frac{y_T-\ell}{(y_T-\ell)^2+h^2}\right]\right\} \qquad (21)$$

Utilizing the requirements of the small aspect ratio assumption

$$|y \pm \ell| < |x \pm b_{1,2}|$$

together with the fact that

$|x_T + b_2| = x_T + b_2$ and that h is extremely small, i.e., $h << 1$ yields

$$W_2 = \frac{-p_o}{\pi\rho U}\left\{\frac{h^2}{x_T+b_2}\left[\frac{1}{y_T+\ell+x_T+b_2} - \frac{1}{y_T-\ell+x_T+b_2}\right]\right.$$

$$- \frac{h^2}{|x_T+b_1|}\left[\frac{1}{y_T+\ell+|x_T-b_1|} - \frac{1}{(y_T-\ell)+|x_T-b_1|}\right]$$

$$\left. - 2\ell\left[|x_T-b_1| - (x_T+b_2) - (b_1+b_2)\right]\left[\frac{1}{y_T^2-\ell^2}\right]\right\} \qquad (22)$$

The above equation holds true only when $h \ll 1$. If $h \to \infty$ (deep water) then it is easily seen that $W_2 \to 0$ (Eq. 21) and the integral equation (12) reduces to that of a planing surface in deep water.

D) Spanwise Lift Distribution

The evaluation of spanwise lift distribution (Eq. 15) requires the integration

$$\Lambda = \int_{-\ell}^{\ell} W(x_T,y')\,\Psi(y_T,y')dy' \qquad (23)$$

which can be considerably facilitated by using the trigonometric transformation

$$y' = -\ell\cos\varphi$$

$$y = -\ell\cos\theta$$

This yields

$$\pi\Psi(y_T, y') = \ell n \left| \frac{1 - \cos\theta\cos\varphi - \sin\theta\sin\varphi}{\cos\theta - \cos\varphi} \right|$$

$$= 2 \sum_{n=1}^{\infty} \frac{\sin n\theta}{n} \sin n\varphi \tag{24}$$

Thus

$$\Lambda = \frac{2\ell}{\pi} \sum_{n=1}^{\infty} \frac{\sin n\theta}{n} \int_0^{\pi} W(x_T, -\ell\cos\varphi) \sin n\varphi \sin\varphi \, d\varphi$$

and finally

$$\Lambda = \Lambda_1 + \Lambda_2 + \Lambda_3 \tag{25}$$

where

$$\Lambda_1 = -\ell U\beta \sin\theta \tag{26}$$

$$\Lambda_2 = -\frac{4p_o}{\pi\rho U} \Big[|x_T - b_1| - (x_T + b_2) - (b_1 + b_2) \Big] \sum_{n=1}^{\infty} \sin n\theta$$

$$\cdot \left\{ 1 - \frac{n^2 - 1^2}{3!2} + \frac{(n^2-1^2)(n^2-3^2)}{5!} \quad \frac{3}{8} \quad \cdot \cdot \cdot \cdot \right\} \text{ for n odd} \tag{27}$$

$$= 0 \text{ for n even}$$

$$\Lambda_3 = -\frac{2p_o h^2}{\pi\rho U} \sum_{n=1}^{\infty} \frac{\sin n\theta}{n} \left\{ \frac{\lambda_1^{\ n}}{x_T + b_2} - \frac{\lambda_2^{\ n}}{x_T + b_2} - \frac{\lambda_3^{\ n}}{|x_T - b_1|} + \frac{\lambda_4^{\ n}}{|x_T - b_1|} \right\} \tag{28}$$

where

$$\lambda_1 = \frac{x_T + b_2 + \ell - \sqrt{(x_T + b_2 + \ell)^2 - \ell^2}}{\ell} \quad \text{provided} \left| \frac{\ell}{\ell + x_T + b_2} \right| \leq 1$$

$$\lambda_2 = \frac{x_T+b_2-\ell+\sqrt{(x_T+b_2-\ell)^2-\ell^2}}{\ell} \quad \text{provided} \quad \left|\frac{\ell}{\ell-(x_T+b_2)}\right| \le 1$$

$$\lambda_3 = \frac{|x_T-b_1|+\ell-\sqrt{(|x_T-b_1|+\ell)^2-\ell^2}}{\ell} \quad \text{provided} \quad \left|\frac{\ell}{\ell+|x_T-b_1|}\right| \le 1$$

(29)

All the provisions are met for the low aspect ratio lifting surface, i.e., $\ell/b < 1$. For λ_4 either

$$\lambda_4 = \frac{|x_T-b_1|-\ell+\sqrt{(|x_T-b_1|-\ell)^2-\ell^2}}{\ell} \tag{30}$$

provided $\left|\frac{\ell}{\ell-|x_T-b_1|}\right| < 1$

or

$$\lambda_4^n = \cos n\psi$$

where

$$\psi = \frac{|x_T-b_1|-\ell}{\ell}$$

provided $\left|\frac{\ell}{\ell-|x_T-b_1|}\right| > 1$ (31)

The first condition for the evaluation of λ_4 is satisfied

for $\frac{b_1}{b} < 1$ and $\frac{b_1}{b} < 1 - 2\frac{\ell}{b}$

or $\frac{b_1}{b} > 1$ and $\frac{b_1}{b} > 1 + 2\frac{\ell}{b}$

whereas the second condition is satisfied for

$$\frac{b_1}{b} < 1 \qquad \text{and} \qquad \frac{b_1}{b} > 1 - \frac{2\ell}{b}$$

or

$$\frac{b_1}{b} > 1 \qquad \text{and} \qquad \frac{b_1}{b} < 1 + \frac{2\ell}{b}$$

Thus the value of λ_4 has two different expressions depending on the imposed geometric condition on both the tire and its footprint. The realizability of the imposed geometric condition can only be decided from experimental observations. As is seen from Figure 12 of Reference (4) the pneumatic tire keeps its symmetrical position with respect to the wheel axle during the entire process from the static condition until the stage of complete detachment. At the final stage the leading edge of the footprint of the hydroplaning tire remains approximately at the same distance from the wheel axle, i.e., $b \sim b_2$, whereas the trailing edge of the lifting surface moves away from its original position towards the wheel axle, i.e., $b_1 > b$.

Under those circumstances λ_4 is given either by Equation 30 when $b_1/b > 1 + 2\frac{\ell}{b}$ or by Equation 31 when $b_1/b < 1 + 2\frac{\ell}{b}$.

E) Total Lift on the Hydroplaning Tire

The total lift can be calculated from Eq. (17) after substitution of Eqs. (25), (26), (27) and (28), so that

$$L = -\rho U \int_{-\ell}^{\ell} \left[\Lambda_1(y_T)+\Lambda_2(b,y_T)+\Lambda_3(b,y_T)\right] dy_T \tag{32}$$

where with $y_T = -\ell\cos\theta$ and $dy_T = \ell\sin\theta\, d\theta$ and $x_T = b$

$$\int_{-\ell}^{\ell} \Lambda_1(y_T)dy_T = -\frac{\pi}{2}\ell^2 U\beta$$

$$\int_{-\ell}^{\ell} \Lambda_2(b,y_T)dy_T = \ell \int_0^{\pi} \Lambda_2(b,-\ell\cos\theta)\sin\theta \, d\theta$$

$$= \frac{2p_o\ell}{\rho U}\Big[|b-b_1| - (b+b_2) - (b_1+b_2)\Big]$$

$$\int_{-\ell}^{\ell} \Lambda_3(b,y_T)dy_T = + \frac{p_o h^2 \ell}{\rho U}\left\{\frac{\lambda_1 - \lambda_2}{b + b_2} - \frac{\lambda_3 - \lambda_4}{|b - b_1|}\right\}$$

Then

$$- L = - \frac{\pi}{2}\rho U^2\ell^2\beta + 2p_o\ell\Big[|b-b_1| - (b+b_2) - (b_1+b_2)\Big]$$

$$+ p_o h^2 \left\{\frac{\ell}{b+b_2}(\lambda_1-\lambda_2) - \frac{\ell}{|b-b_1|}(\lambda_3-\lambda_4)\right\} \qquad (33)$$

Letting $\ell/b = A$ (aspect ratio) then

$$\frac{\ell}{b+b_2}(\lambda_1-\lambda_2) = \frac{2A}{1+b_2/b} - \sqrt{1 + \frac{2A}{1+b_2/b}} - \sqrt{1 - \frac{2A}{1 + b_2/b}} \qquad (34)$$

and when

$$\left|\frac{A}{A - |1-b_1/b|}\right| < 1 \quad ,$$

$$- \frac{\ell}{|b-b_1|}(\lambda_3-\lambda_4) = \frac{-2A}{|1 - b_1/b|} \mp \sqrt{1 - \frac{2A}{|1-b_1/b|}} + \sqrt{1 + \frac{2A}{|1-b_1/b|}} \qquad (35)$$

or when

or when

$$\left| \frac{A}{A - |1 - b_1/b|} \right| > 1 ,$$

$$- \frac{\ell}{|b-b_1|} (\lambda_3 - \lambda_4) = \frac{-2A}{|1-b_1/b|} + \sqrt{1 + \frac{2A}{|1-b_1/b|}} \tag{36}$$

If the lift coefficient is defined as

$$C_L = \frac{-L}{\frac{1}{2} \rho U^2 (2b)(2\ell)} \tag{37}$$

and use is made of the fact that at the hydroplaning stage the force exerted on the ground must be balanced by the force exerted on the tire, i.e.,

$$\frac{p_o}{\frac{1}{2} \rho U^2} = - \frac{C_L}{2} \frac{2b}{b_1 + b_2}$$

where the factor $\frac{1}{2}$ (of C_L) is introduced to account for the depth correction suggested by Wadlin and Christopher in Reference (9), then Eqs. (33) to (37) yield

$$C_L = - \frac{\pi}{4} AB - \frac{C_L}{2(b_1+b_2)} \left[|b-b_1| - (b+b_2) - (b_1+b_2) \right]$$

$$- C_L \left(\frac{h}{2\ell}\right)^2 \frac{A}{b_1/b + b_2/b} F(A)$$

or

$$C_L = \frac{-\frac{\pi}{4} A \beta}{1 + \frac{\left[|b-b_1| - (b+b_2) - (b_1+b_2)\right]}{2(b_1+b_2)} + \left(\frac{h}{2\ell}\right)^2 \frac{A}{\frac{b_1}{b} + \frac{b_2}{b}} F(A)}$$

where

1) for $\left| \frac{A}{A - |1-b_1/b|} \right| < 1$ (38)

$$F(A) = F_1(A) = \frac{2A}{1+b_2/b} - \sqrt{1 + \frac{2A}{1+b_2/b}} - \sqrt{1 - \frac{2A}{1+b_2/b}}$$

$$- \frac{2A}{|1-b_1/b|} + \sqrt{1 + \frac{2A}{|1-b_1/b|}} + \sqrt{1 - \frac{2A}{|1-b_1/b|}}$$

2) and for $\left| \frac{A}{A - |1-b_1/b|} \right| > 1$

$$F(A) = F_2(A) = \frac{2A}{1+b_2/b} - \sqrt{1 + \frac{2A}{1+b_2/b}} - \sqrt{1 - \frac{2A}{1+b_2/b}}$$

$$- \frac{2A}{|1-b_1/b|} + \sqrt{1 + \frac{2A}{|1-b_1/b}}$$

When $b_1 < b$,

$$\frac{\left[|b-b_1| - (b+b_2) - (b_1+b_2)\right]}{2(b_1 + b_2)} = -1$$

and

$$C_L = - \frac{\frac{\pi}{4} A\beta}{(\frac{h}{2\ell})^2 \frac{A}{b_1/b+b_2/b} F(A)} \tag{39}$$

where

$$F(A) = \begin{cases} F_1(A) & \text{when } b_1/b < 1 - 2A \\ F_2(A) & \text{when } b_1/b > 1 - 2A \end{cases}$$

When $b_1 > b$,

$$\frac{\left[| b-b_1| - (b+b_2) - (b_1+b_2)\right]}{2(b_1+b_2)} = - \frac{b + b_2}{b_1 + b_2}$$

and

$$C_L = - \frac{\frac{\pi}{4} A \beta}{\frac{b_1-b}{b_1+b_2} + (\frac{h}{2\ell})^2 \frac{Ab}{b_1+b_2} F(A)} \tag{40}$$

where

$$F(A) = \begin{cases} F_1(A) & \text{when } b_1/b > 1 + 2A \\ F_2(A) & \text{when } b_1/b < 1 + 2A \end{cases}$$

The orientation and position of the planing tire relative to the runway is more conveniently described in terms of leading and trailing edge clearance (h and d, respectively) and aspect ratio A, rather than angle of attack β and leading edge clearance h. As is seen from Figure 3B, the angle β in radians can be expressed as follows:

$$\beta \approx (1 - \frac{d}{h}) (\frac{h}{2\ell})A \tag{41}$$

Equation (39) or (40) should be used in conjunction with (41) in evaluating the lift coefficient in the hydroplaning stage.

NUMERICAL CALCULATIONS AND DISCUSSION OF RESULTS

The purpose of this preliminary investigation is to devolop a theoretical approach to the hydroplaning of a pneumatic tire from the standpoint of inviscid hydrodynamics. The theory furnishes an expression for the lift coefficient in terms of the aspect ratio of the wetted portion of the hydroplaning tire, the geometry of the footprint, the shape of the deflected tire in contact with the water, its position relative to the pavement, and the depth of water on the runway.

In this first attempt the wetted portion of the tire is approximated by a rigid plate of small aspect ratio and the pressure distribution on the ground footprint is assumed to be represented by a uniform distribution in step-like fashion in both directions (longitudinal and transverse) with amplitude equal to that of the internal pressure of the pneumatic tire in accordance with experimental evidence. Thus the problem reduces to that analogous to planing of a small aspect ratio surface on extremely shallow water, when its effect on the bottom (runway) is approximated in this way.

A) Effects of Various Parameters

A series of calculations has been performed for a variety of tire positions relative to the runway at different depths of water with various tire aspect ratios and footprint geometry. These systematic calculations bring out the relative importance of the various parameters which describe the hydroplaning phenomenon from the standpoint of hydrodynamics. Furthermore, generally favorable qualitative comparison of the results with those of experiments under similar conditions strengthens the validity of the mathematical model and substantiates the primary assumption that the problem is a hydrodynamical one. It should be kept in mind that the results must be used only for a qualitative description of the hydroplaning tire, since the problem has been analyzed only approximately.

Figures 4 and 5 present the computed total lift coefficient C_L of a planing tire in terms of depth of water, h, for various aspect ratios, A, and at various heights, d, of the trailing edge of the tire above the ground. The tire has been assumed to be a rigid flat surface planing at a fixed trim angle defined by Equation (41). Figure 4 is for a ratio of ground footprint area to horizontal projected tire wetted area of 1.17, while Figure 5 is for an area ratio of 1.25. In both cases it is assumed that the leading edges of the footprint and tire lie on the same perpendicular line, i.e., $b_2 = b$ whereas the trailing edge of the footprint is aft of the trailing edge of the hydroplaning tire. In the first case $b_1/b = 4/3$ and in the second $b_1/b = 3/2$. The curves exhibited in Figures 4 and 5 can be considered to represent the boundary between the hydroplaning and non-hydroplaning regimes. In fact, they represent the lift coefficient C_{L_i}, at incipient hydroplaning. Thus if C_L of a given tire configuration with known loading and footprint geometry can be estimated, then the condition $C_L \lesseqgtr C_{L_i}$ (i.e., smaller or greater than lift coefficient of incipient hydroplaning) at a given depth of water on the runway will determine whether or not the tire will hydroplane under these conditions. Several interesting results are evident from an examination of Figures 4 and 5 -- these are described below.

Effect of Aspect Ratio (A): For a given thickness of water layer, h, and height, d, of tire trailing edge above the runway, there is a rapid increase in hydroplaning lift coefficient as the aspect ratio, A, is increased. This effect is particularly evident as the water layer thickness is increased. The normal aspect ratio of aircraft tires is of the order of 0.75. Thus it appears to be of some benefit to reduce the tire aspect ratio so as to obtain smaller planing lift coefficients and hence higher speeds of planing inception.

Effect of Water Depth (h): For a given aspect ratio and tire height above the runway, it is seen, in Figures 4 and 5, that the planing lift coefficient increases rapidly with increasing water depth h -- this is especially true for the larger values of aspect ratio. Hence, all other conditions being equal, the possibility of hydroplaning increases significantly with increasing thickness of water layer. This conclusion is not considered to be at variance with the results of the experimental program described by Dugoff and Ehrlich,[11] since there are more constraints imposed on the theoretical variations than in the experiments. The length of the footprint for example, which appears to have a great effect, was held constant as $h/2\ell$ was varied in the calculations while in the experiments this parameter is necessarily allowed to take on any value.

Effect of Tire Clearance (d): For a given aspect ratio and water depth, there is a relatively small decrease in lift coefficient for rather large increases in tire clearance -- especially for high aspect ratios and large water depths. For example, at water depth $h/2\ell = .30$, and aspect ratio 0.80, the lift coefficient decreases only 20% for a 500% increase in ground clearance (from $d/h = 0.05$ to $d/h = 0.30$). Since the hydroplaning speed varies inversely as the square root of the planing lift coefficient, the speed of incipient hydroplaning will increase only about 10% for a 500% increase in ground clearance, all other factors being equal. For a given set of environmental conditions then, these results indicate that the lift coefficient will be nearly constant during hydroplaning.

To illustrate this point further, Figures 6 and 7 have bee prepared to show the relative importance of tire clearance and water depth on C_L. For a wide range of aspect ratios it is seen that, to maintain a constant C_L of either 0.7 or 0.8, a 500% increase in tire clearance d/h corresponds to only a 10-15% increase in water depth $h/2\ell$ or a 5-10% decrease in wetted area of the tire. This indicates that once tire hydroplaning occurs it is rather insensitive to ground clearance so that a nearly constant C_L results for a given h and A. In fact, experimental data (Ref. 4,5) and two-dimensional theory (Ref. 1) do indicate an essentially constant C_L during hydroplaning for a wide range of d/h values.

Effect of Footprint/Tireprint Area Ratio (b_1/b): Figure 4 presents results for $b_1/b = 4/3$ while the results in Figure 5 are for $b_1/b = 3/2$. It is interesting to note that as the trailing edge of the footprint moves farther aft (b_1/b increasing) C_L decreases or hydroplaning speed increases. Also the family of parametric curves is "stretched" towards greater depth of water on the runway and the stretching is more pronounced with smaller aspect ratio.

It is interesting to compare the results of the present analysis with the experimental results of Christopher (Ref. 10) who studies the effect of shallow water on the hydrodynamic characteristics of a flat planing surface. Among his experimental configurations those with clearances $d/2\ell = 0.20$ to 0.25, for a range of A, are selected for comparison with the present theory because they represent more closely the conditions of the mathematical model. The theoretical calculations were performed for values of $b_1/b = 2$ based on Christopher's experimental observation that the roach of the wake moves aft of the trailing edge of the flat plate as the depth of the water is increased. As is seen from Figure 11 of Ref. 10, the roaching of the streamline aft of the test model is accompanied by a pronounced trough which, in turn, indicates the extent of the high pressure region aft of the surface. It is believed that the wake of a flat planing surface in shallow water will extend much farther aft than that of a tire with the same aspect ratio and with its characteristic curvature when hydroplaning in extremely shallow water. The comparison with theoretical results is exhibited in Figure 8. It is seen that theory and experiment are in satisfactory agreement for small values of A up to 0.4 for the entire range of $h/2\ell$. As A increases, the region of favorable agreement moves towards smaller values of $h/2\ell$. However, it should be noted that if a higher value of b_1/b had been taken for the higher aspect ratio range, the agreement would have been better.

B) Inception of Hydroplaning

The previous results can be used to predict hydroplaning inception speeds. Equating the integrated pressure load on the runway to the integrated pressure load on the tire

$$p_o(b_1 + b_2)2\ell = \tfrac{1}{2}\,\rho U^2\,\frac{C_L}{2}\cdot 2b\cdot 2\ell$$

results in

$$U_{inception} = \sqrt{\frac{2p_oK}{C_L}} \tag{42}$$

where p_o is the tire pressure in lb/ft^2, $K = (b_1 + b_2)/2b$, $\rho/2 \approx 1$.

For given values of environmental conditions, i.e., h, A, K, it has been previously shown experimentally, that C_L is essentially constant so that the inception speed of planing is proportional to the square root of tire pressure. This result is in accordance with the experimental observations of Reference (4,5). Theoretically, however, the constancy of C_{L_i} for all conditions cannot be explained as yet.

To compare the present theoretical results with experimental data, the planing inception speed has been computed for the test conditions reported in Figure 4 of Reference (4) and summarized in the Table below.

Table 1

Planing Parameters of Tires of Reference 1

Tire No.	D, in. diam.	W, in. width	$2\ell^*$, in. = .84W	$2b^*$, in. = .44D	A = ℓ/b	h, in. water depth	$\frac{h}{2\ell}$	P_o lb/in^2
1a	32	8.8	7.4	14.1	0.52	0.65	0.088	115
1b	32	8.8	7.4	14.1	0.52	1.0	0.135	90
2	44	13.0	10.9	19.4	0.56	0.1	0.009	130
3	49	17.0	14.3	21.6	0.66	0.4	0.028	65
4	39	13.0	10.9	17.2	0.63	0.3	0.027	150
5a	38	12.5	10.5	16.7	0.62	0.3	0.028	25
5b	38	12.5	10.5	16.7	0.62	0.3	0.028	50
5c	38	12.5	10.5	16.7	0.62	0.3	0.028	75
6a	28	6.7	5.6	12.3	0.45	0.3	0.053	25
6b	28	6.7	5.6	12.3	0.45	0.3	0.053	40

*Estimated by the method of Reference (6).

Since the experiments were conducted in extremely shallow water (h less than one inch), the lift coefficients were calculated for two additional values of b_1/b, 1.1 and 1.03. These are shown in Figures 9 and 10.

The values of estimated hydroplaning inception speed U_i are compared below with the experimental values reported in Reference (4).

Table 2

Experimental U_i and U_i Estimated by the Present Theory for $b_1/b = 1.1$ and $b_1/b = 1.03$

Tire No.	D in.	W in.	U_i ft/sec exp	U_i, ft/sec, estimated from	
				$b_1/b = 1.1$	$b_1/b = 1.03$
1a	32	8.8	160	236	-*
1b	32	8.8	132	111	-*
2	44	13.0	175	808	472
3	49	17.0	120	304	93
4	39	13.0	200	473	166
5a	38	12.5	67	193	67
5b	38	12.5	100	273	95
5c	38	12.5	120	334	116
6a	28	6.7	86	193	-*
6b	28	6.7	100	244	-*

*Cannot be estimated for these combinations of b_1/b, A and $h/2\ell$.

This comparison indicates that with a proper choice of b_1/b it is possible to obtain the experimental speed of hydroplaning inception. It is apparent that b_1/b is a very decisive parameter for the description of the mathematical model, and furthermore that b_1/b must be a function of depth h of the water film on the runway, tire clearance, d, speed of advance, etc. As the depth decreases, b_1 approaches b; in other words, the area of ground pressure comes closer to the wetted area of the hydroplaning tire.

The results presented in Table 2 confirm again the validity of the basic assumption that the hydroplaning tire phenomenon can be studied from the standpoint of inviscid hydrodynamics. However, they also point up the shortcomings of the present approximate theory in its inability to specify b_1/b. It could be argued that the agreement is fortuitous and therefore the results should be used only for guidance and qualitative description of the phenomenon. It is desirable therefore to extend the present study of the hydroplaning tire so as to evaluate accurately the three-dimensional hydrodynamic effect in this phenomenon.

CONCLUSIONS

An approximate theory has been developed for studying the hydroplaning tire by considering it as a planing surface of small aspect ratio in extremely shallow water. The results obtained on the basis of this approximation exhibit hydrodynamic behavior similar to that of a hydroplaning pneumatic tire and furnish some qualitative guidance for avoiding this undesired condition.

The present approximate theory indicates that the phenomenon of hydroplaning of a tire can be described from the standpoint of inviscid hydrodynamics. The analysis furnishes families of curves which determine the boundary between the hydroplaning and non-hydroplaning condition, depending on the geometry of the planing surface, its position relative to the runway, the geometry of the footprint pressure distribution and the depth of water on the runway. These curves which can be considered to represent "incipient hydroplaning" establish criteria for avoiding the undesired hydroplaning condition. Theory indicates specifically that:

a) Avoidance of hydroplaning is extended to higher depth of water for smaller aspect ratios, whereas for high aspect ratio hydroplaning can be avoided only for smaller depths.

b) Constancy of the lift coefficient can be obtained with a large number of combinations of aspect ratios, depth of water on the runway and clearance (gap) of the trailing edge of the lifting surface from the ground.

c) Increasing values of clearance (gap) yield decreasing values of C_L.

d) Even when there is a drastic increase in values of clearances the lift coefficient remains constant with unnoticeable changes of the wetted portion of the pneumatic tire or depth of water on the runway.

e) As the horizontal distance of the trailing edge of the hydroplaning tire moves closer to the perpendicular through the axle, the possibility of avoiding the hydroplaning condition is extended to higher depth of water.

Interpreting these results from the viewpoint of speed at which hydroplaning starts yields the following fundamental conclusions:

a) The incipient hydroplaning speed U_i decreases with increasing aspect ratio or increasing depth of water. A given large value of U_i is attained either by smaller aspect ratio at larger depth of water or larger aspect ratio at smaller depth of water.

b) Increasing values of clearance (gap) yield increasing values of speed of incipient hydroplaning.

c) Hydroplaning of a tire can be delayed or avoided by increasing U_i which can be achieved by decreasing the aspect ratio of the wetted surface.

Finally, it should be emphasized that the results must be used merely as a qualitative description of the hydroplaning tire, since the problem has been analyzed only approximately on the basis of two assumptions: a) the wetted surface of the tire is a low aspect ratio planing surface and b) the pressure distribution on the ground can be approximated by a uniform step-function.

For future studies it is recommended to undertake the task of evaluating accurately the three-dimensional hydrodynamic effect in the hydroplaning of the tire before attempting to incorporate the elasticity of the tire in the mathematical model. It would also be advisable, as a check on the theory, to conduct a set of experiments with rigid flat plates to simulate the flat-plate planing conditions treated theoretically. This can be done at Davidson Laboratory on the existing simulator for testing tires in the hydroplaning stage.

ACKNOWLEDGEMENT

The authors are indebted to Mr. Daniel Savitsky, Manager of the Applied Mechanics Group of Davidson Laboratory, for his valuable suggestions.

REFERENCES

1. Martin, C.S.: "Hydrodynamics of Tire Hydroplaning," NASA CR-601, September 1966

2. Moore, D.F.: "A Study of Tire-Surface Interaction for the Case of Rolling on a Wet Surface," Cornell Aero. Lab. Report YD-1969-V-2, 1965

3. Gross, W.A., Stahler, A. and Wildman, M.: "A Comparison of Characteristics of Self-Acting Foil Bearings and Pneumatic Tires," Ampex Report RB 65-32, 1965

4. Horne, W.B. and Dreher, R.C.: "Phenomena of Pneumatic Tire Hydroplaning," NASA TN D-2056, November 1963

5. Horne, W.B. and Joyner, U.T.: "Pneumatic Tire Hydroplaning and Some Effects on Vehicle Performance," Soc. Automotive Eng., 970 C, January 1965

6. Smiley, R.F. and Horne, W.B.: "Mechanical Properties of Pneumatic Tires with Special Reference to Modern Aircraft Tires," NASA TR-R-64, 1960

7. Tsakonas, S. and Henry, C.J.: "Finite Aspect Ratio Configurations in a Free Surface Wave System," DL Report 1118, June 1966

8. Watkins, C.E., Woolston, D. and Cunningham, H.: "A Systematic Kernel Function Procedure for Determining Aerodynamic Forces on Oscillating or Steady Finite Wings at Subsonic Speeds," NASA TR-R-48, 1959

9. Wadlin, K.L. and Christopher, K.W.: "A Method for Calculation of Hydrodynamic Lift for Submerged and Planing Rectangular Lifting Surfaces," NASA-TR-R-14, 1959

10. Christopher, K.W.: "Effect of Shallow Water on the Hydrodynamic Characteristics of a Flat-Bottom Planing Surface," NACA Tech. Note 3642, April 1956

11. Dugoff, H. and Ehrlich, R., "Laboratory-Scale Model Experiments to Investigate Aircraft Tire Hydroplaning," Proceedings of the 7th Annual Conference on Environmental Effects on Aircraft and Propulsion Systems, September 1967.

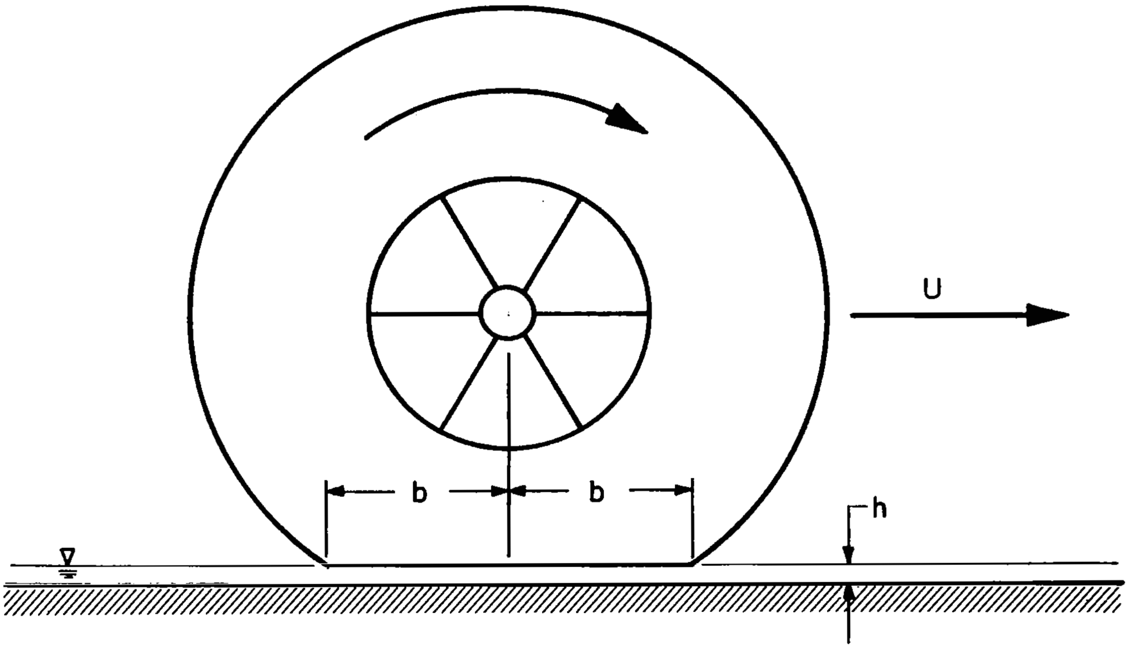

FIGURE 1. PNEUMATIC TIRE AT HYDROPLANING STAGE

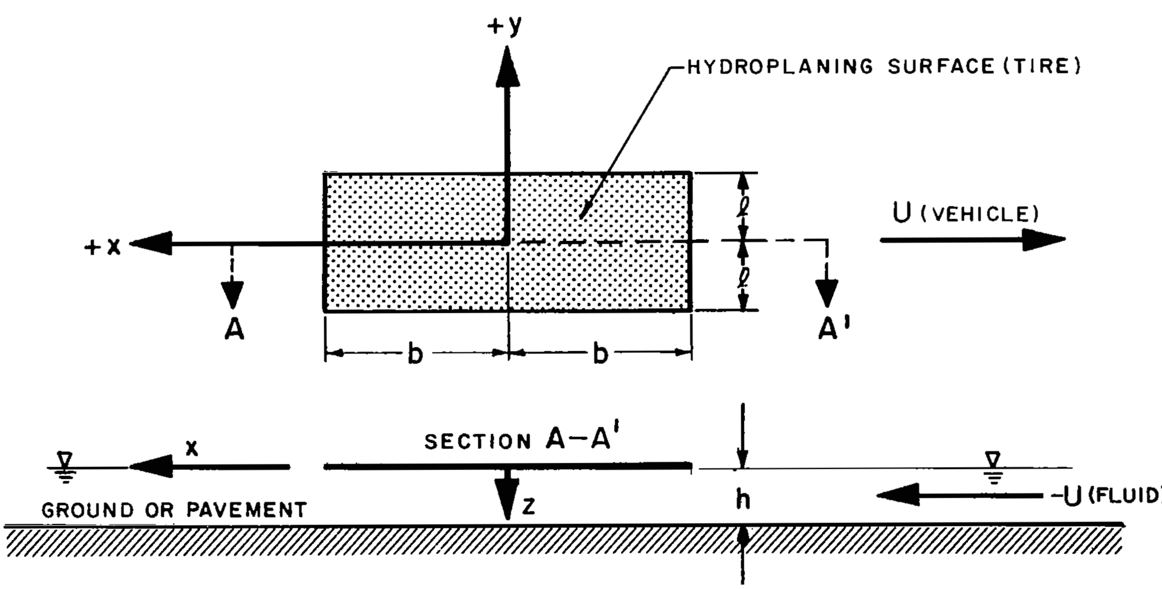

FIGURE 2. HYDRODYNAMIC EQUIVALENT OF HYDROPLANING TIRE

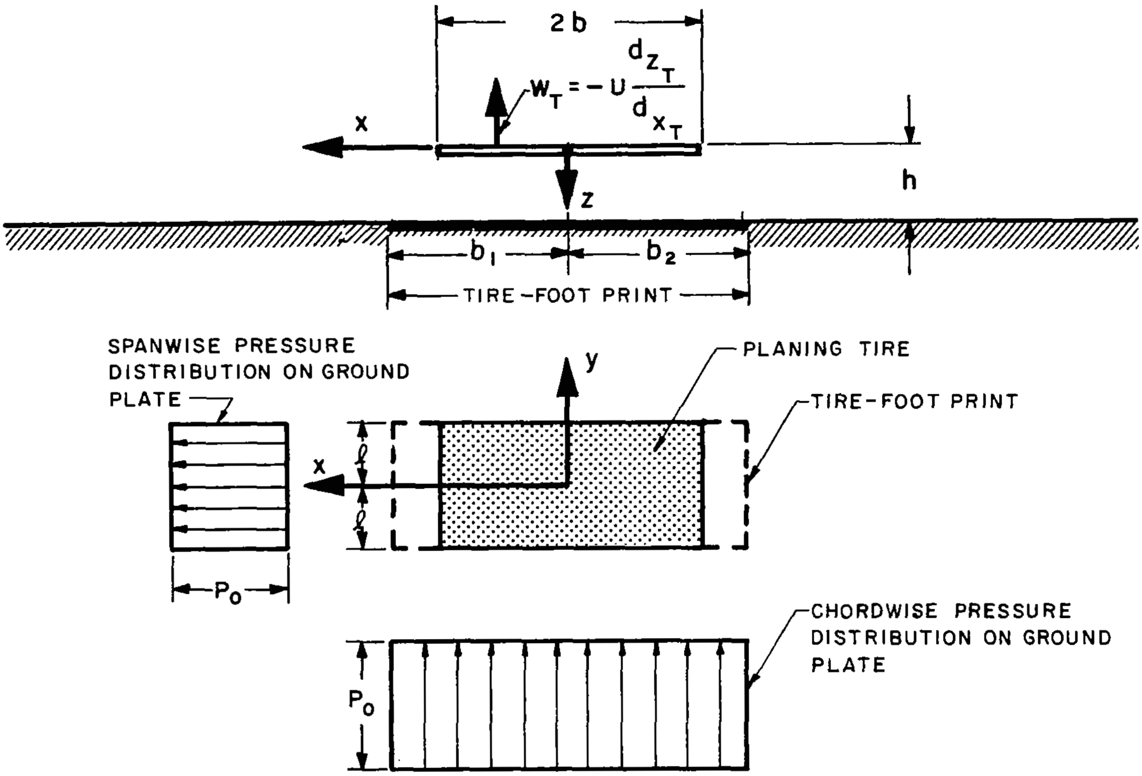

FIGURE 3A. REPRESENTATION OF SIMPLIFIED MATHEMATICAL MODEL

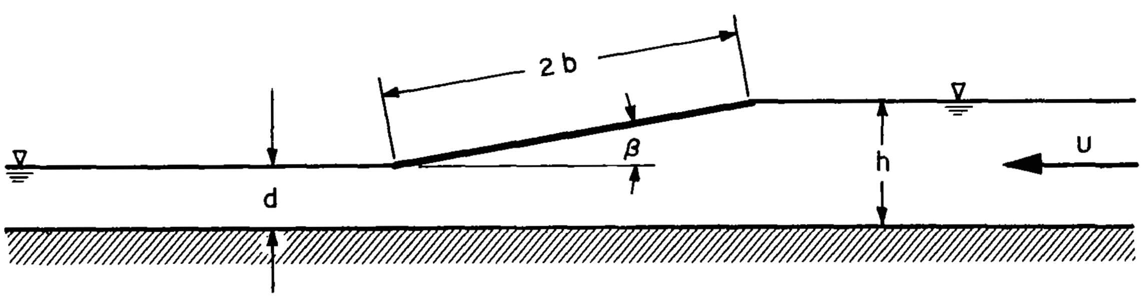

FIGURE 3B. POSITION OF PLANING SURFACE RELATIVE TO RUNWAY

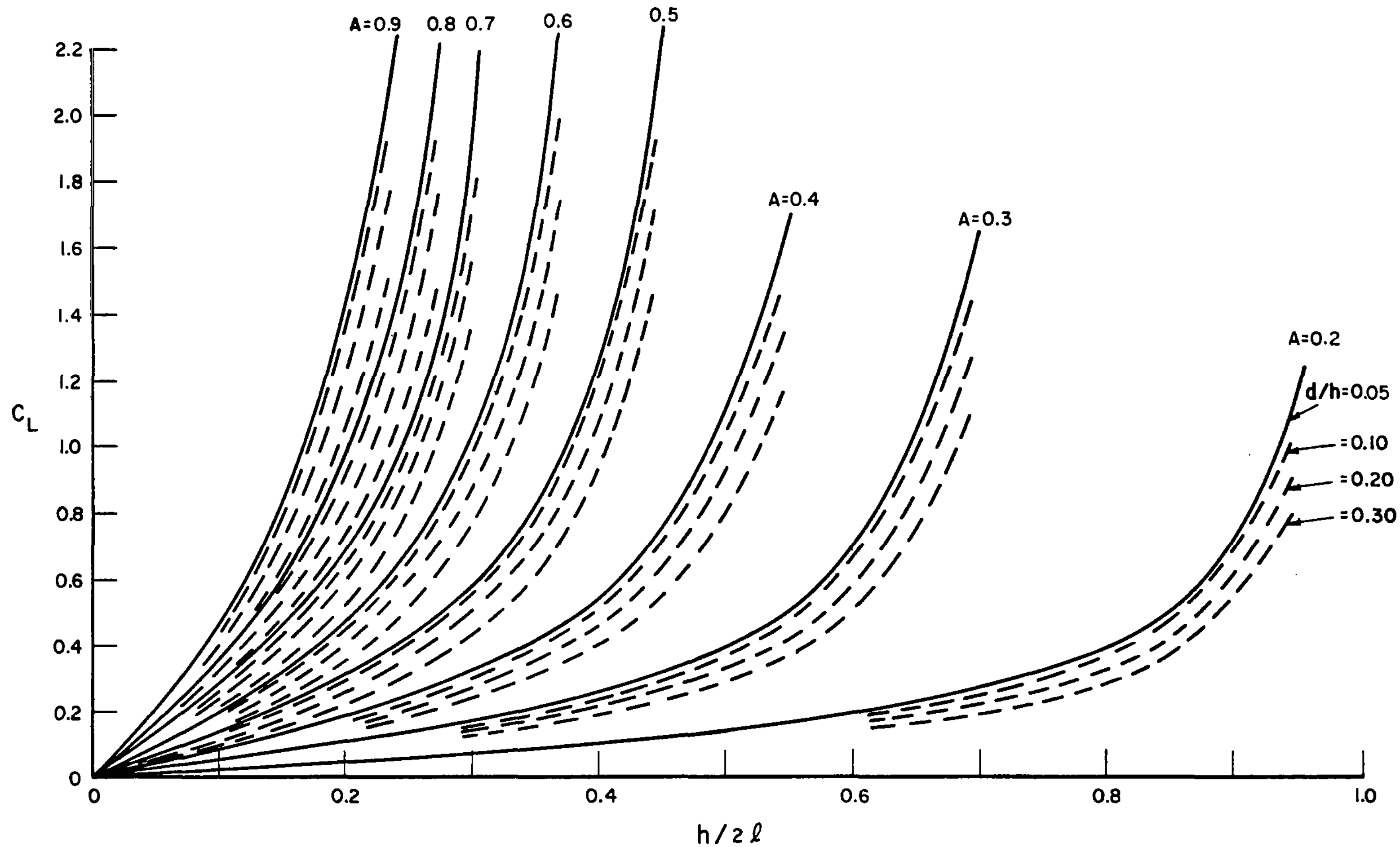

FIGURE 4. LIFT COEFFICIENT OF HYDROPLANING TIRE IN TERMS OF h, d AND A ASSUMING $b_1/b = 4/3$

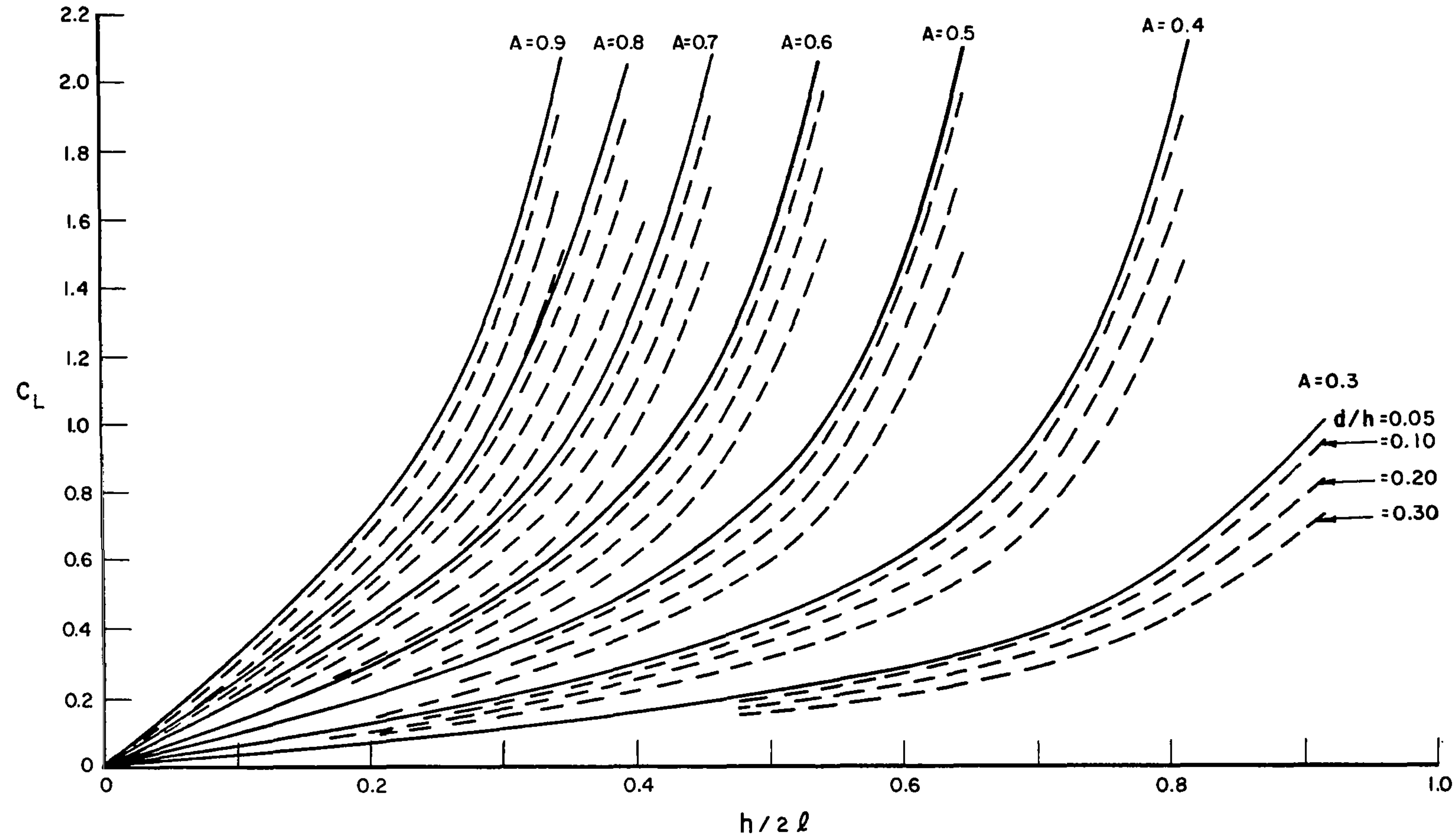

FIGURE 5. LIFT COEFFICIENT OF HYDROPLANING TIRE IN TERMS OF h, d AND A ASSUMING $b_1/b = 3/2$

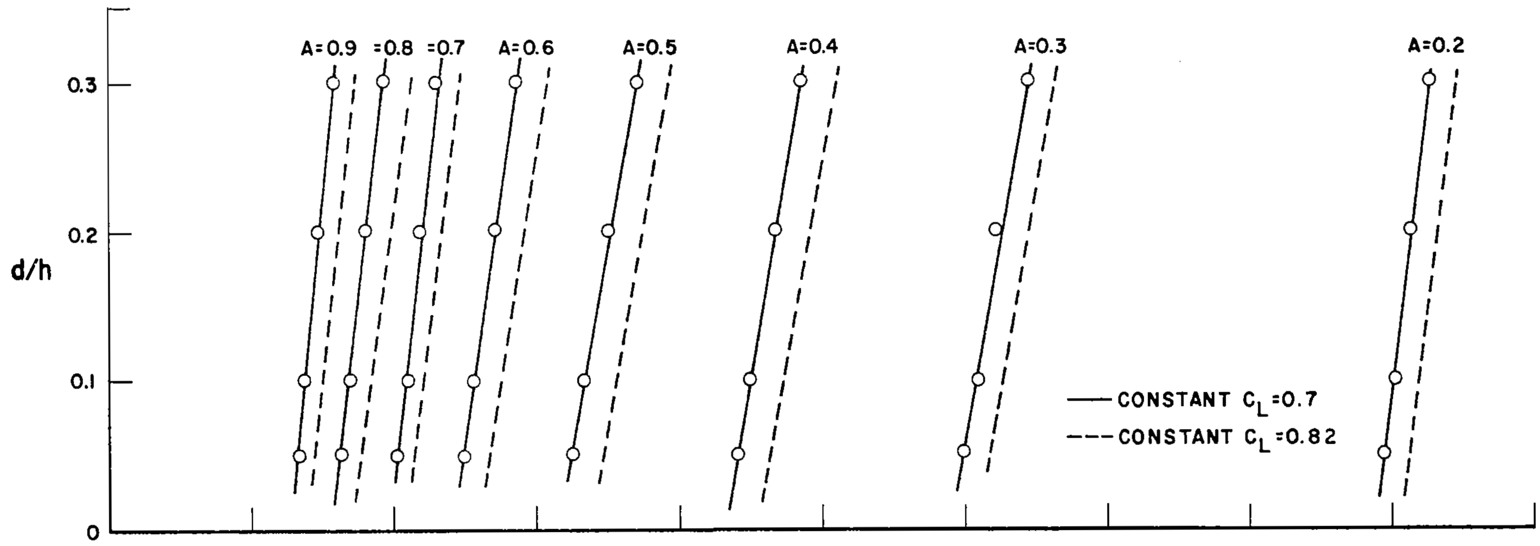

FIGURE 6. CLEARANCE d IN TERMS OF h AND A FOR CONSTANT C_L AND $b_1/b = 4/3$

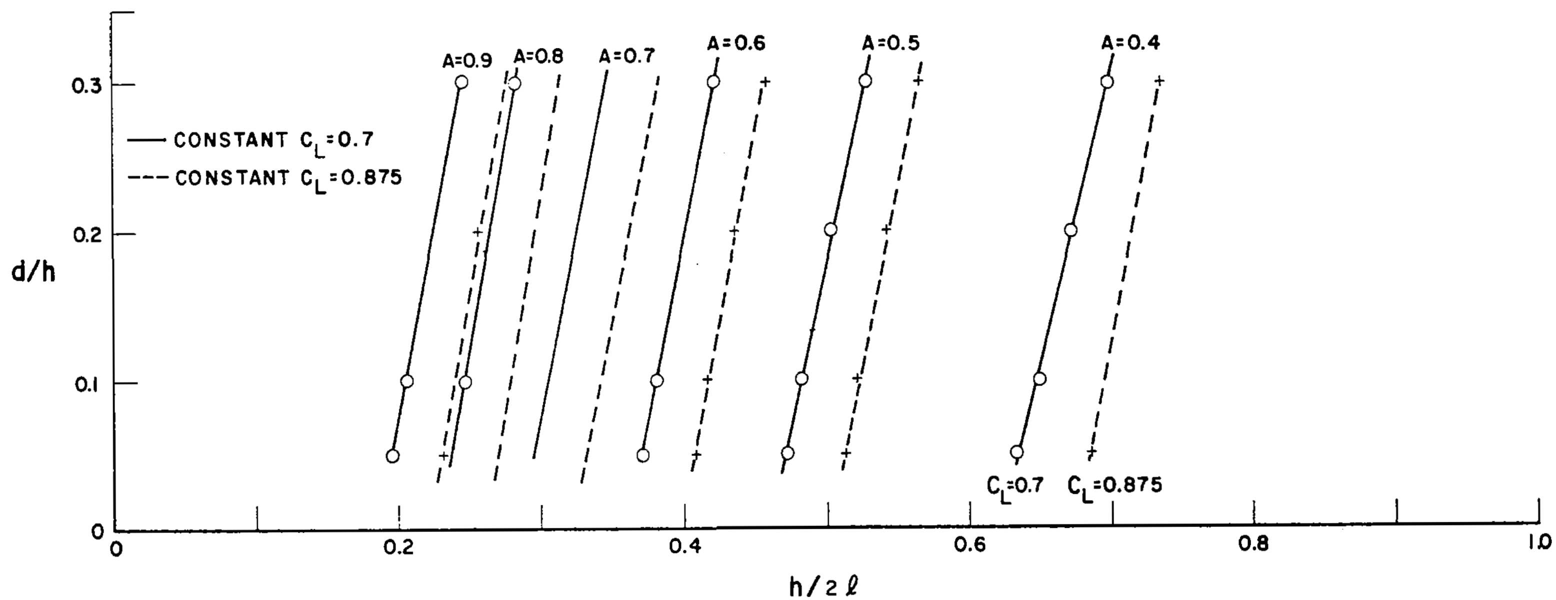

FIGURE 7. CLEARANCE d IN TERMS OF h AND A FOR CONSTANT C_L AND $b_1/b = 3/2$

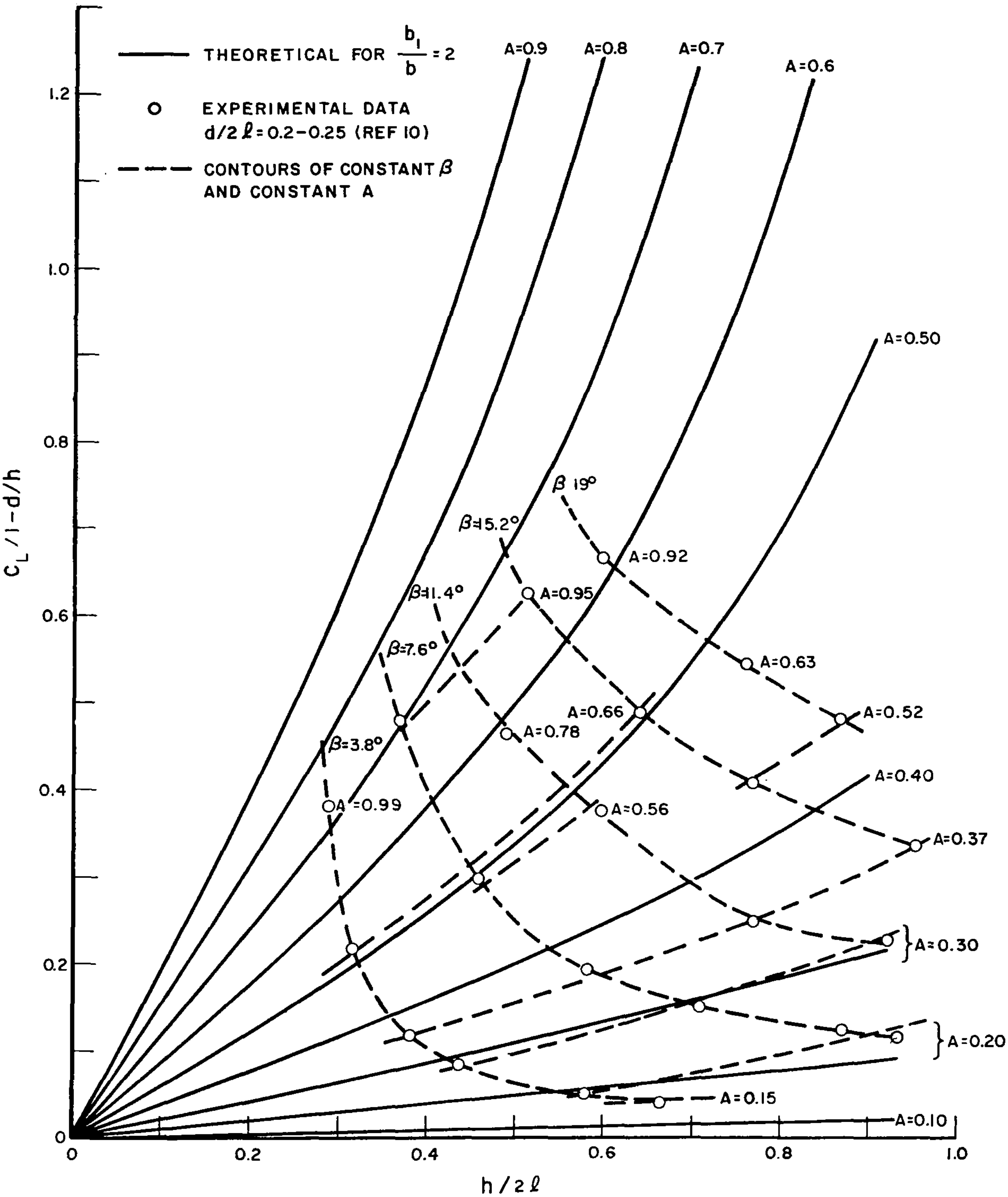

FIGURE 8. COMPARISON OF THEORETICAL LIFT COEFFICIENTS FOR $b_1/b=2$ WITH EXPERIMENTAL DATA FOR FLAT PLANING SURFACES (REF. 10)

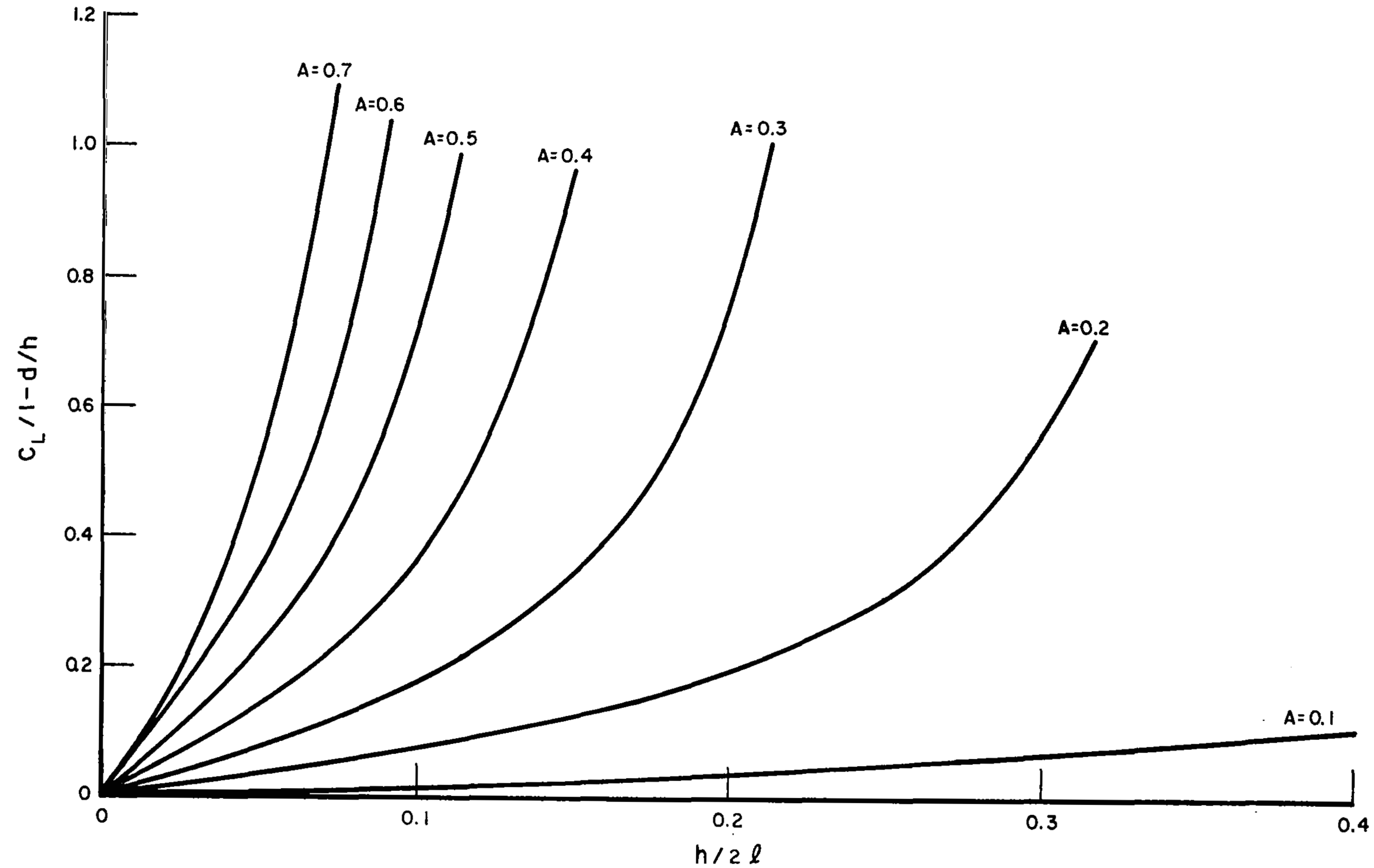

FIGURE 9. LIFT COEFFICIENT OF HYDROPLANING TIRE IN TERMS OF h AND A ASSUMING $b_1/b = 1.1$

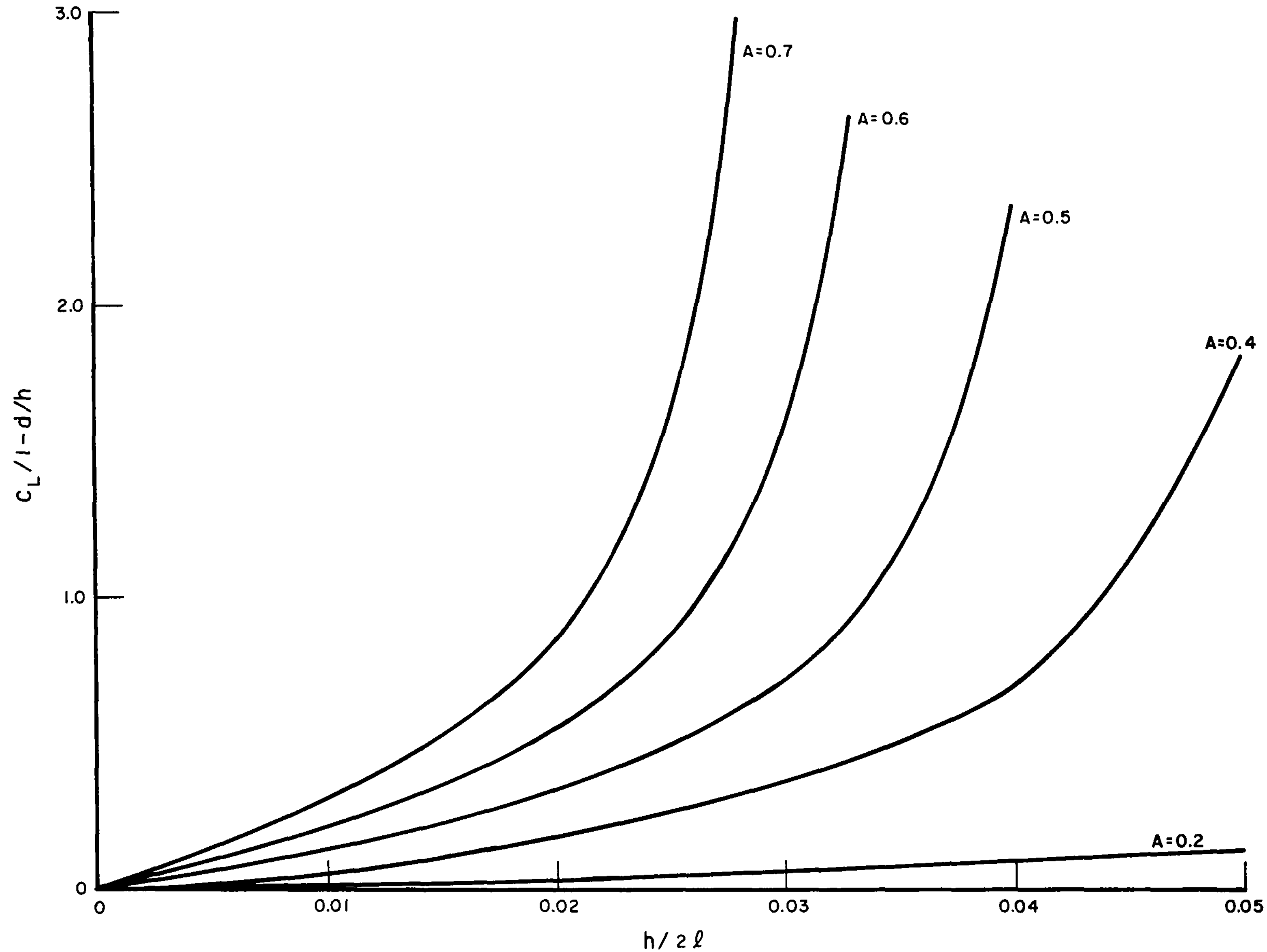

FIGURE 10. LIFT COEFFICIENT OF HYDROPLANING TIRE IN TERMS OF h AND A ASSUMING $b_1/b = 1.03$

APPENDIX A

The solution of the integral equation

$$f(z) = \int_{-\ell}^{\ell} \varphi(\zeta) \frac{\partial}{\partial z} \left(\frac{1}{z-\zeta}\right) d\zeta \tag{A-1}$$

is known in the literature. For the sake of completeness of this study, however, a derivation of the solution is presented here which was independently arrived at by the authors.

The form of the kernel function in Eq. (A-1) suggests integration by parts. This yields

$$f(z) = -\varphi(\zeta) \frac{1}{z-\xi}\Bigg|_{-\ell}^{\ell} + \int_{-\ell}^{\ell} \frac{d\varphi}{d\zeta} \frac{1}{z-\zeta}\, d\zeta$$

With the assumption that

$$\varphi(\ell) = \varphi(-\ell) = 0 \tag{A-2}$$

which, in fact, corresponds to the desired tip conditions, the result is

$$f(z) = \int_{-\ell}^{\ell} \frac{d\varphi}{d\zeta} \frac{1}{z-\zeta}\, d\zeta \tag{A-3}$$

The auxiliary condition

$$\int_{-\ell}^{\ell} \frac{d\varphi}{d\zeta}\, d\zeta = \varphi\Bigg|_{-\ell}^{\ell} = 0$$

resulting from the assumed tip condition (A-2) secures a unique solution of the integral equation (A-3) with Cauchy-type singular kernel. The solution is given by

$$\frac{d\varphi}{dz} = -\frac{1}{\pi^2} \frac{1}{\sqrt{\ell^2 - z^2}} \int_{-\ell}^{\ell} \frac{f(\zeta)\sqrt{\ell^2 - \zeta^2}}{z - \zeta}\, d\zeta$$

or

$$\varphi(z) = -\frac{1}{\pi^2}\int_{-\ell}^{z}\frac{1}{\sqrt{\ell^2 - z^2}}\int_{-\ell}^{\ell}\frac{f(\zeta)\sqrt{\ell^2 - \zeta^2}}{z - \zeta}\,d\zeta \tag{A-4}$$

Since interchanging the order of integration is permissible for a Cauchy kernel, the z-integration is performed first:

$$\int_{-\ell}^{z}\frac{dz}{\sqrt{\ell^2 - z^2}(z-\zeta)} = -\frac{1}{\sqrt{\ell^2 - \zeta^2}}\log\frac{\ell^2 - z\zeta + \sqrt{(\ell^2 - z^2)(\ell^2 - \zeta^2)}}{\ell(\zeta - z)}$$

Hence, Eq. (A-4) reduces to

$$\varphi(z) = \frac{1}{\pi^2}\int_{-\ell}^{\ell} f(\zeta)\log\frac{\ell^2 - z\zeta + \sqrt{(\ell^2 - z^2)(\ell^2 - \zeta^2)}}{\ell(\zeta - z)}\,d\zeta \tag{A-5}$$

APPENDIX B

When the low aspect ratio assumption is abandoned, the integral equation (9) will be shown to reduce to the Fredholm integral equation of the second kind.

The integral equation can be written as

$$\frac{1}{\pi}\int_{-\ell}^{\ell}\frac{L'(b,\eta)}{(y-\eta)^2}\,d\eta = 2\rho UW - \frac{1}{\pi}\int_{-\ell}^{\ell}\frac{d\eta}{(y-\eta)^2}\int_{-b}^{x}L(\xi,\eta)\frac{x-\xi}{\sqrt{(x-\xi)^2+(y-\eta)^2}}\,d\xi \tag{B-1}$$

If the inner integral is integrated by parts by identifying

$$u = \frac{x-\xi}{\sqrt{(x-\xi)^2+(y-\eta)^2}} \quad \text{and} \quad dv = L(\xi,\eta)d\xi$$

so that

$$du = -\frac{(y-\eta)^2\,d\xi}{\left[(x-\xi)^2+(y-\eta)^2\right]^{3/2}} \quad \text{and} \quad v = \int_{-b}^{\xi}L(\xi',\eta)d\xi' = L'(\xi,\eta) \tag{B-2}$$

then it becomes

$$\frac{x-\xi}{\sqrt{(x-\xi)^2+(y-\eta)^2}}L'(\xi,\eta)\Bigg|_{-b}^{x} + \int_{-b}^{x}L'(\xi,\eta)\frac{(y-\eta)^2}{\left[(x-\xi)^2+(y-\eta)^2\right]^{3/2}}d\xi$$

$$= \int_{-b}^{x}L'(\xi,\eta)\frac{(y-\eta)^2}{\left[(x-\xi)^2+(y-\eta)^2\right]^{3/2}}d\xi$$

The integral equation can then be written as

$$\int_{-\ell}^{\ell}\frac{L'(b,\eta)}{(y-\eta)^2}\,d\eta = 2\pi\rho UW - \int_{-\ell}^{\ell}\int_{-b}^{x}\frac{L'(\xi,\eta)}{\left[(x-\xi)^2+(y-\eta)^2\right]^{3/2}}\,d\xi d\eta \tag{B-3}$$

Multiplying both sides of Eq. B-3 by the ψ-function (see Eq. 16) and integrating with respect to y' over the range $-\ell$ to ℓ yields

$$L'(b,\eta) = 2\rho\pi U\int_{-\ell}^{\ell}W(b,y')\Psi(y,y')dy' - \int_{-\ell}^{\ell}\int_{-b}^{x}L'(\xi,\eta)\bar{K}(x,y;\xi,\eta)d\xi d\eta$$

which is the Fredholm integral of the second kind where

$$\bar{K}(x,y;\xi,\eta) = \int_{-\ell}^{\ell} \frac{1}{\left[(x-\xi)^2 + (y'-\eta)^2\right]^{3/2}} \Psi(y,y')dy'$$

and $L'(\xi,\eta)$ is the unknown function to be determined.

NASA-Langley, 1968 —— 12 CR-1125